out for both compounds with the wavelengths $\lambda = 1.7965(1)$ and $\lambda = 1.3066(1)$ Å in the range $2^\circ < 2\theta < 158^\circ$. Crystal structure data for SrN_2 at 298 K derived from neutron diffraction experiments: tetragonal, space group *I*4/*mmm* (no. 139), $a = 3.8136(3)$, $c = 6.2855(4)$ Å, $V = 91.4(1)$ Å^3, $Z = 2$; Sr in (2a); N in (4e), $z = 0.4026(2)$; $R_{profile} = 0.0422$, $R_{Bragg} = 0.0358$; number of observed reflections: 61. Crystal structure data for SrN at 298 K from neutron diffraction experiments: monoclinic, space group *C*2/*m* (12), $a = 13.472(1)$, $b = 3.8121(3)$, $c = 6.7284(5)$ Å, $\beta = 94.720(1)^\circ$, $V = 344.4(1)$ Å^3, $Z = 8$, Sr1 in (4i) $x = 0.1541(3)$, $z = 0.3926(7)$; Sr2 in (4i) x = 0.3561(4), $z = 0.0922(6)$; N1 in (4i) $x = 0.2442(3)$, $z = 0.7487(6)$; N2 in (4i) $x = 0.0223(3)$, $z = 0.0830(6)$; $R_{profile} = 0.0527$, $R_{Bragg} = 0.0663$; number of observed reflections: 690. The refinements have been carried out using the programs WinPLOTR[8] and FULLPROF.[9] The following scattering lengths were used: Sr 7.02 fm; N 9.36 fm.[10] Further details on the crystal structure investigations may be obtained from the Fachinformationszentrum Karlsruhe, 76344 Eggenstein-Leopoldshafen, Germany (fax: (+49) 7247-808-666; e-mail: crysdata@fiz-karlsruhe.de), on quoting the depository numbers CSD-411555, and CSD-411556.

[7] D. M. Többens, N. Stüßer, K. Knorr, H. M. Mayer, G. Lampert, *Proceedings 7th European Powder Conference*, **2000**, in press.

[8] T. Roisnel, J. Rodriguez-Carvajal, Laboratoire Léon Brillouin, WinPLOTR, Version May, **2000**.

[9] J. Rodriguez-Carvajal, Laboratoire Léon Brillouin, FULLPROF.2k, Version 1.6, **2000**.

[10] V. F. Sears, *Neutron News* **1992**, *3*, 26.

[11] Yu. Prots, G. Auffermann, W. Schnelle, D. Többens, R. Kniep, unpublished results.

[12] The nonmetallic components (N, O, H, C) were quantitatively determined by carrier-gas-hot-extraction or combustion techniques (TC 436 DR/5, RH 404 and C-200 CHLH (LECO)): SrN [N exp. 13.9(2) wt %, calcd 13.84 wt %]; SrN_2 [N exp. 24.5(2) wt %, calcd 24.23 wt %]. Impurities of O, H, and C were not detected [detection limits: C < 0.1 wt %, H < 0.005 wt %, O < 0.05 wt %]. In $(Sr^{2+})_4[N^{3-}]_2[N_2^{2-}]$, the existence of two different nitrogen species with the molar ratio 1:1 became obvious by temperature ramping (700 – 800 K) during the determination of the nitrogen content. As expected, only one maximum was observed for $Sr^{2+}[N_2^{2-}]$ and $(Sr^{"1.5+"})_2[N^{3-}]$ indicating the evidence of only one nitrogen species in each case.

[13] a) V. Vohn, M. Knapp, U. Ruschewitz, *J. Solid State Chem.* **2000**, *151*, 111 – 116; b) O. Reckeweg, A. Baumann, H. A. Mayer, J. Glaser, H.-J. Meyer, *Z. Anorg. Allg. Chem.* **1999**, *625*, 1686 – 1692.

[14] R. R. Schrock, R. M. Kolodziej, A. H. Liu, W. M. Davis, M. G. Vale, *J. Am. Chem. Soc.* **1990**, *112*, 4338 – 4345.

[15] D. Sellmann, W. Soglowek, F. Knoch, M. Moll, *Angew. Chem.* **1989**, *101*, 1244 – 1245.

[16] The formation of diazenides in the system Ba – N was reported by G. Vajenine (Department Prof. A. Simon, Max-Planck-Institut für Festkörperforschung, Stuttgart) at the "Hemdsärmelkolloquium" (17.03.2000) in Dresden.

Dendron-Controlled Nucleation and Growth of Gold Nanoparticles**

Ruiyao Wang, Jun Yang, Zhiping Zheng,*
Michael D. Carducci, Jun Jiao, and Supapan Seraphin

Nanoclusters of metals and semiconductors—which exhibit unusual size-dependent electronic, magnetic, optical, and catalytic properties due to the onset of "quantum effects"—are being heralded as the next generation of building blocks for designing modern materials.[1] However, these particles are metastable and cannot be isolated or manipulated without appropriate stabilization by organic capping ligands.[2] Various functionalized organic arrays including protein cages,[3] polymer matrices,[4] and surfactant vesicles[5] have been used previously to form nanoparticles by encapsulation. A more recent development is the use of polyamidoamine (PAMAM) dendrimers[6]—a class of highly branched, monodisperse, and globular synthetic polymers—to passivate nanoclusters of zero-valent metals,[7] metal oxides,[8] and metal sulfides.[8, 9] However, a simple relationship between particle size and dendrimer generation was not established.[10]

In contrast to classical dendrimers such as the PAMAM species, a dendron is a segment of dendrimer that possesses a focal point onto which the branching units of a dendritic architecture are attached.[11] If the focal moiety is capable of metal complexation, the specific metal – dendron interactions can be utilized to control reactions at this site.[12] We envision that such reactivity control in a confined and localized area may be used for the controlled growth and stabilization of nanoparticles. Such a concept is validated here with the production of gold nanocrystals using dendrons G1 – G3 with a focal 4-pyridone functionality[13] as capping agents.

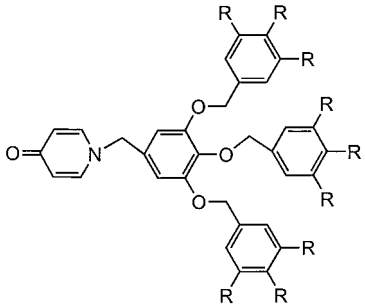

G1 R = H

G2 R = $OCH_2C_6H_5$

G3 R = OCH_2 with $OCH_2C_6H_5$ groups

[*] Prof. Dr. Z. Zheng, Dr. R. Wang, Dr. J. Yang, Dr. M. D. Carducci
Department of Chemistry
University of Arizona
Tucson, AZ 85721 (USA)
Fax: (+1) 520-621-8407
E-mail: zhiping@u.arizona.edu

Dr. J. Jiao, Prof. Dr. S. Seraphin
Department of Materials Science and Engineering
University of Arizona, Tucson, AZ (USA)

[**] We thank the University of Arizona and the Research Corporation for financial support. Acknowledgement is also made to the donors of the Petroleum Research Fund, administered by the American Chemical Society, for partial support of this research. The X-ray diffractometer was purchased with support from the U.S. National Science Foundation (CHEM-9610374). We thank Dr. K. Nebesny for help with the XPS experiments.

Supporting information for this article is available on the WWW under http://www.angewandte.com or from the author.

  1433-7851/01/4003-0549 $ 17.50+.50/0

The gold–dendron nanocomposites were synthesized by the liquid–liquid phase-transfer reaction[14] shown in Equation (1) (Gn = nth-generation dendron; n = 1–3). In all cases,

$$HAuCl_4 + (n\text{-}C_8H_{17})_4NBr + Gn + NaBH_4 \rightarrow Au{-}Gn \quad (1)$$

wine-red solutions were obtained. These solutions exhibit a characteristic gold surface plasmon (SP) resonance at about $\lambda = 525$ nm (Figure 1) and are stable for at least six months

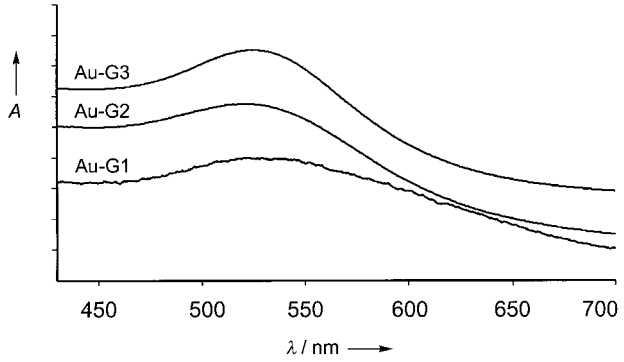

Figure 1. UV/Vis spectra of solutions of nanocomposites Au–Gn (n = 1–3). The absorbance A is arbitrarily normalized at $\lambda = 450$ nm.

under ambient conditions. This stability is attributable to passivation of the metal surface by the dendrons, as only insoluble black residues were obtained in the absence of the capping ligands. A similar wine-red solution can also be generated without using any phase-transfer agent, however, with a significant amount of black precipitate. This is presumably due to the inefficient mixing of $HAuCl_4/NaBH_4$ with the dendrons in the absence of the agent. These observations lead to the conclusion that the use of a phase-transfer agent facilitates formation of the gold–dendron composites, but is not mandatory.

The gold–dendron nanocomposites can be isolated from the solution as dark crystalline solids that redissolve in dichloromethane without noticeable visual changes. Further purification by recrystallization from dichloromethane/pentane yields analytically pure Au–G1 and Au–G2, but Au–G3 is contaminated with a small amount of free G3 due to similar solubilities. Microanalysis of Au–G1 revealed its composition to be 5% G1 and 95% Au, corresponding roughly to an Au:G1 ratio of 49:1. Based on the packing density calculation for bulk-state gold,[15] a 2-nm particle (see below) contains 247 gold atoms, leading to the formula $Au_{247}(G1)_5$. A straightforward calculation[16] gives an $Au_{surface}$:G1 ratio of 27.5:1, which is not unreasonable considering the coverage offered by the umbrella-shaped dendron.

Transmission electron microscopy (TEM) analysis (Figure 2) of the dropcast films of Au–Gn demonstrates the correlation between the particle size and the generation number of the dendron: The higher the generation, the larger the encapsulated particles. Thus, with G1, G2, and G3 gold particles with an average diameter of 2.0 ± 1.0, 3.3 ± 1.1, and 5.1 ± 1.7 nm (measured over 200 particles in each case) were obtained, respectively. The characteristic [111] gold lattice fringes (inset, Figure 2a) manifest crystallinity of the particles.

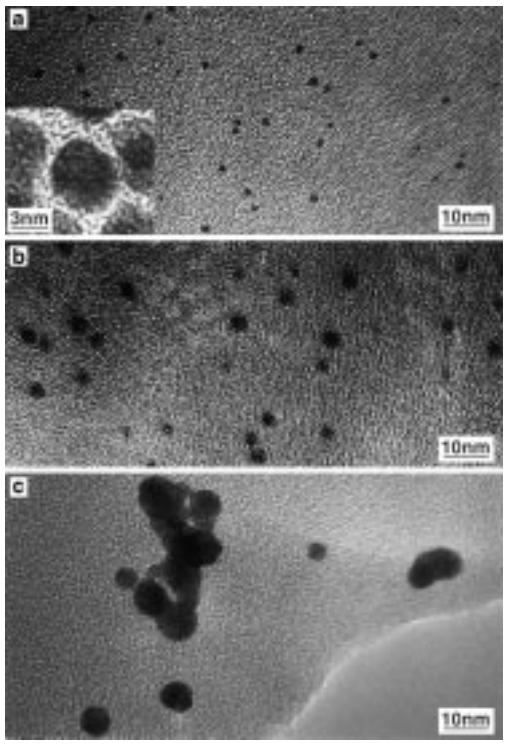

Figure 2. Transmission electron micrographs of a) Au–G1, b) Au–G2, and c) Au–G3. Inset: gold lattice fringence of Au–G1.

The TEM images of differently sized particles were corroborated by the UV/Vis absorption spectra of the particle solution: Going from Au–G3 to Au–G1, the SP band blue shifts slightly (3 nm) and decreases in intensity with decreasing particle size. Similar trends were observed for Au nanocrystals stabilized by PAMAM dendrimers.[7c,d, 10]

Before the size control imposed by different-generation dendrons can be rationalized, the microscopic interactions between the dendron and the gold surface need to be discerned. The dendron focal moiety appears to be the only reasonable site where the particles may nucleate and grow, because the dendron surface lacks metal-stabilizing groups, while the loose dendron may not be able to sustain the confinement of the particles within the branching units. The N atom, the C=O moiety, and even the conjugated six-membered ring can potentially bind metals. Efforts have been made to establish the dendron coordination mode(s), but definitive assignment of a particular type of dendron–gold interaction is difficult owing to the intrinsically weak nature of such interactions. The IR spectra of Au–G1 and Au–G2 are essentially superimposible with those of their respective ligands. This observation is in line with results reported for the similarly weak PAMAM–gold interactions.[7c, 17]

The ^{1}HNMR signals of Au–G2, though significantly broadened, appear at positions that are almost identical to those of free G2. Similar observations are well documented for gold nanoparticles functionalized with passivating amines[16] and thiols,[2a] and the broadening effects have been extensively discussed.[2a] The XPS studies revealed noticeable broadening of 1s peaks for C, O, and N atoms in Au–G2 relative to free G2, but the changes in ionization energies are

  1433-7851/01/4003-0550 $ 17.50+.50/0

negligible, indicating a rather weak interaction between the metal surface and individual dendrons. Based upon these observations, the possibility of N–Au and focal ring–Au interactions cannot be ruled out. However, such modes of particle stabilization, both involving the seemingly inaccessable N atom, are less likely due to steric encumbrance. The C=O moiety is therefore putatively responsible for binding to the metal, and the observed passivation is provided by the dendron sheath within which the single gold particle resides (Figure 3). To the best of our knowledge, there are no

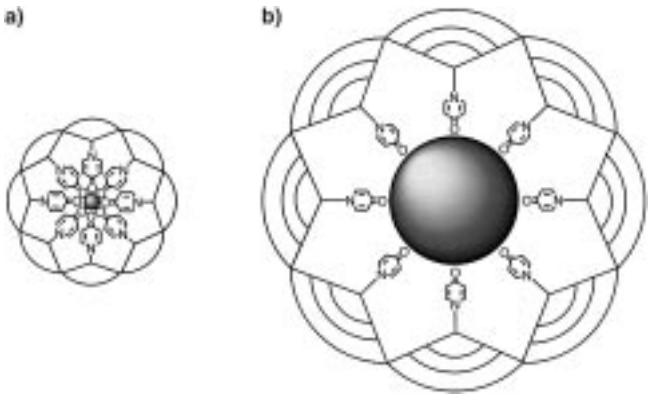

Figure 3. Schematic presentation of Au–G*n* nanocrystallite growth controlled by different-generation dendrons: a) G1 and b) G3.

precedents for monolayer formation of pyridone derivatives on bulk metal surfaces of any kind, presumably due to the chemical instability of such monolayers. This work thus represents an exciting departure from the bulk systems in that the high surface curvature (as a result of their finite size) of the Au nanoparticles supports the high-density packing of the capping ligands, which provide concomitant protection of the nanocrystals.[16]

The systematic variation of particle size may be understood as follows: The higher the dendron generation, the greater the steric requirement of the focal metal-binding moiety, and hence the more room for gold atoms to agglomerate (Figure 3). This steric argument can be easily appreciated by comparing the bulk of a G2 dendron (nine peripheral aromatic rings, Figure 4[18]) with that of a G1 dendron (only three peripheral aromatic rings). Given the weak force between the particle and the dendrons, particle aggregation conceivably occurs, and the nanocomposite containing the more sterically demanding dendrons is more susceptible to such a coalescence. In other words, the more hindered periphery leads to a less compact and therefore less stable composite structure because of the increasing open space between the branching units. This hypothesis is corroborated by the observation that the particles of Au–G3 (Figure 2c) are not as well separated as those of Au–G1 (Figure 2a) and Au–G2 (Figure 2b). Dendrons with a focal thiol group would be more propitious for stabilizing gold nanoparticles and therefore mitigating particle agglomeration. Experiments with such dendrons are in progress as are studies of other factors that possibly affect the particle size and size distribution (for example, dendron:metal ratio, rate of reductant addition, and reaction temperature).

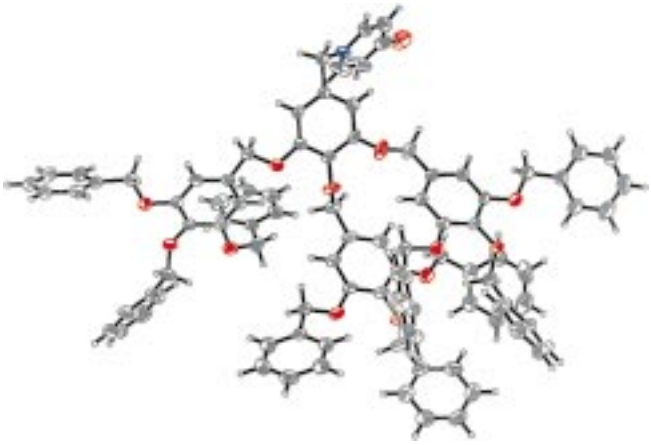

Figure 4. An ORTEP representation of the crystal structure of G2 at the 50% probability level. Carbon: gray, nitrogen: blue, oxygen: red.

In summary, we have demonstrated that dendrons that are focally modified with a metal-coordinating functionality can be utilized as stabilizing media for the controlled growth of nanocrystals. With 4-pyridone-based dendrons, gold nanoclusters were obtained that are stable for six months both in solution and in the solid state. The average size of the resulting nanoparticles is a direct function of the generation number of the passivating dendron, with higher generation dendrons producing larger particles.

Experimental Section

To a solution of $HAuCl_4 \cdot 3H_2O$ (11.2 mg, 28.4 μmol) in deionized water (5 mL) was added $(n\text{-}C_8H_{17})_4NBr$ (36.5 mg, 66.7 μmol) in toluene/CH_2Cl_2 (15 mL, 2/1). An orange-red organic phase and a colorless aqueous phase resulted after 1 h of vigorous stirring. The dendron (310 μmol; 0.156, 0.452, and 1.34 g for G1, G2, and G3, respectively) in CH_2Cl_2 (15 mL) was added to the above mixture. Subsequent dropwise addition of a freshly prepared aqueous solution (5 mL) of $NaBH_4$ (16.5 mg, 436 μmol) caused an instant color change of the mixture to wine-red. The resulting mixture was stirred under dry N_2 for an additional 24 h. Decanting the aqueous phase and adding ethanol to the organic phase at $-20\,^{\circ}C$ afforded the products as dark purple solids. Recrystallization from CH_2Cl_2/pentane yielded dark purple crystalline solids (Au–G1 and Au–G2) or dark purple waxy solids (Au–G3). Elemental analysis of Au–G1: C 4.14, H 0.25, N 0.14. Based on this CHN analysis and the molecular formula of G1 ($C_{33}H_{29}NO_4$), O is calculated to make up 0.64% of the Au–G1 nanocomposite, and hence Au makes up 94.8%.

Received: May 15, 2000
Revised: November 7, 2000 [Z15126]

[1] A. P. Alivisatos, *Endeavor* **1997**, *21*, 56–60.
[2] a) A. C. Templeton, W. P. Wuelfing, R. W. Murray, *Acc. Chem. Res.* **2000**, *33*, 27–36, and references therein; b) *Clusters and Colloids: From Theory to Applications* (Ed.: G. Schmidt), VCH, Weinheim, **1994**.
[3] a) T. Douglas, M. J. Young, *Nature* **1998**, *393*, 152–155; b) F. C. Meldrum, B. R. Heywood, S. Mann, *Science* **1992**, *257*, 522–523.
[4] a) D. H. Cole, K. R. Shull, P. Baldo, L. Rehn, *Macromolecules* **1999**, *32*, 771–777; b) R. F. Zilo, E. P. Giannelis, B. A. Weinstein, M. P. O'Hara, B. N. Ganguly, V. Mehrotra, M. W. Russell, D. R. Huffman, *Science* **1992**, *257*, 219–223.

  1433-7851/01/4003-0551 $ 17.50+.50/0

[5] a) M. P. Peleni, J. Tanori, A. Felakembo, J. C. Dedieu, T. Gulik-Krzywicki, *Langmuir* **1998**, *14*, 7359 – 7363; b) S. Mann, J. P. Hannington, R. J. P. Williams, *Nature* **1986**, *324*, 565 – 567.

[6] G. R. Newkome, C. N. Moorefield, F. Vögtle, *Dendritic Molecules: Concepts, Synthesis, Perspectives*, VCH, Weinheim, **1996**.

[7] a) M. Zhao, L. Sun, R. M. Crooks, *J. Am. Chem. Soc.* **1998**, *120*, 4877 – 4878; b) L. Balogh, D. A. Tomalia, *J. Am. Chem. Soc.* **1998**, *120*, 7355 – 7356; c) M. E. Garcia, L. A. Baker, R. M. Crooks, *Anal. Chem.* **1999**, *71*, 256 – 258; d) K. Esumi, A. Suzuki, N. Aihara, K. Usui, K. Torigoe, *Langmuir* **1998**, *14*, 3157 – 3159.

[8] L. Balogh, D. R. Swanson, R. Spindler, D. A. Tomalia, *Polym. Mater. Sci. Eng.* **1997**, *77*, 118 – 119.

[9] K. Sooklal, L. H. Hanus, H. J. Ploehn, C. J. Murphy, *Adv. Mater.* **1998**, *10*, 1083 – 1087.

[10] F. Gröhn, B. J. Bauer, E. J. Amis, *Polym. Prepr. Am. Chem. Soc. Div. Polym. Chem.* **2000**, *41*, 560 – 561.

[11] a) J. M. J. Fréchet, *Science* **1994**, *263*, 1710 – 1715; b) H. Frey, *Angew. Chem.* **1998**, *110*, 2313 – 2318; *Angew. Chem. Int. Ed.* **1998**, *37*, 2193 – 2197.

[12] G. R. Newkome, E. He, C. N. Moorefield, *Chem. Rev.* **1999**, *99*, 1689 – 1746.

[13] R. Wang, Z. Zheng, *J. Am. Chem. Soc.* **1999**, *121*, 3549 – 3550. On the basis of our X-ray diffraction analyses, the dendrons based on 4-alkoxypyridine reported previously were incorrectly formulated and are restructured as having a focal 4-pyridone moiety.

[14] M. Brust, M. Walker, D. Bethell, D. J. Schiffrin, R. Whyman, *Chem. Commun.* **1994**, 801 – 802.

[15] M. M. Alvarez, J. T. Khoury, T. G. Schaaff, M. N. Shafigullin, I. Vezmar, R. L. Whetten, *J. Phys. Chem. B* **1997**, *101*, 3706 – 3712.

[16] D. V. Leaf, L. Brandt, J. R. Heath, *Langmuir* **1996**, *12*, 4723 – 4730.

[17] H. Tokuhisa, M. Zhao, L. A. Baker, V. T. Phan, D. L. Dermody, M. E. Garcia, R. F. Peez, R. M. Crooks, T. M. Mayer, *J. Am. Chem. Soc.* **1998**, *120*, 4492 – 4501.

[18] Crystallographic data for dendron G2: A colorless crystal (ca. $0.09 \times 0.09 \times 0.39$ mm) grown from a solution in acetone was analyzed with a Bruker SMART 1000 CCD-based diffractometer at 170(2) K with $Mo_{K\alpha}$ radiation ($\lambda = 0.71073$ Å). Triclinic, space group $P\bar{1}$, $a = 10.9321(10)$, $b = 18.5767(17)$, $c = 20.6645(19)$ Å, $\alpha = 112.723(2)^\circ$, $\beta = 93.433(2)^\circ$, $\gamma = 91.132(2)^\circ$, $V = 3859.7(6)$ Å^3, $Z = 2$, $\rho_{calcd} = 1.255$ Mg m^{-3}, $\mu(Mo_{K\alpha}) = 0.083$ mm^{-1}, $F(000) = 1540$. $\omega - 2\theta$ scans. Of 45437 reflections measured ($2\theta_{max} = 50^\circ$), 17341 were independent and 6879 observed [$I = 2\sigma(I)$]; 992 refined parameters, $R = 0.0490$, $wR^2 = 0.0917$; max./min. residual electron density 0.297/ − 0.246 e Å^{-3}, max./min. transmission 0.839/0.671. Data reduction was performed using the SAINT software, which corrects for Lp and decay. Absorption corrections were applied using SADABS supplied by G. Sheldrick (Universität Göttingen). The structure was solved by direct methods using SHELXS in Bruker SHELXTL (version 5.0). All non-hydrogen atoms were refined anisotropically, and all hydrogens were calculated by geometrical methods and refined using a riding model. Crystallographic data (excluding structure factors) for the structure reported in this paper have been deposited with the Cambridge Crystallographic Data Centre as supplementary publication no. CCDC-144260. Copies of the data can be obtained free of charge on application to CCDC, 12 Union Road, Cambridge CB2 1EZ, UK (fax: (+44) 1223-336-033; e-mail: deposit@ccdc.cam.ac.uk).

Alkylene-bridged *N,N,N′N′* – Tetrasubstituted Bis(2-amino-5-thiazolyl)methinium Salts— A New Class of Strongly Fluorescent Dyes**

Horst Hartmann* and Antje Noack

Owing to their strong fluorescence, pyronines **2a** ($R^1 = H$)[1] and rhodamines **2a** ($R^1 = Aryl$)[2] have found several practical applications, such as fluorescence and laser dyes,[3] or, if they are specifically functionalized, for example at the amino groups, as fluorescence markers for biological substrates and polymer characterization.[4] The fluorescence of the dyes **2a** is in sharp contrast to their unbridged di- and triarylmethane

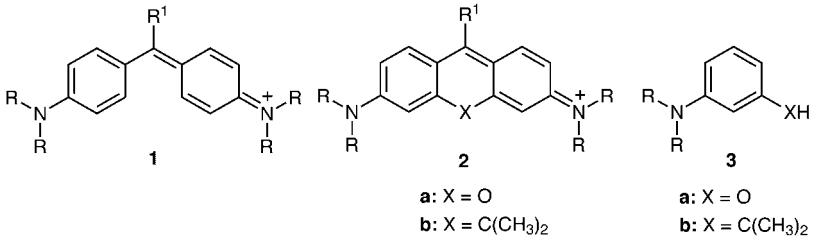

dye analogues **1** which are nonfluorescent under normal conditions.[5] The fluorescence-enhancing effect of bridging by heteroatoms is associated, however, with a pronounced hypsochromism of the absorption of these dyes. Thus, the bridged di- and triarylmethane dyes **2a** absorb at about 550 nm. This is a nearly 50 nm shorter wavelength than the absorption wavelength of their unbridged analogous **1**.[6]

Whereas the fluorescence-enhancement is effected by the increasing rigidity of the molecular system and originates from a restriction or diminishing of the nonradiative deactivation processes[7] the hypsochromic effect originates from the incorporation of the lone pair of the bridging oxygen atom into the conjugation of the π system responsible for the color. This incorporation gives rise to a stabilization of the electronic ground state and, hence, to a widening of the gap between the ground and first excited state in the bridged compounds.[6]

In agreement with this postulate no hypsochromic effect is observed in going from the unbridged compounds **1** to the alkylene-bridged di- and triarylmethane dyes **2b** in which the bridging group has no lone pair. Therefore, these compounds absorb at nearly the same wavelength as their unbridged analogues **1**, but in contrast they exhibit, analogous to the oxygen-bridged compounds **2a**, a strong fluorescence.[8a] A practical application of the isopropylidene-bridged dyes **2b** has not been reported because the necessary educts for these compounds, the isopropylidene-substituted *N,N*-dialkylanilines **3b**, can only be prepared by a multistep reaction from commercially available precursors, making them far less

[*] Prof. Dr. H. Hartmann, Dr. A. Noack
Fachbereich Chemie der Fachhochschule Merseburg
Geusaer Strasse, 06217 Merseburg (Germany)
Fax: (+49) 3461-462192
E-mail: Horst.Hartmann@cui.fh-merseburg.de

[**] This work was supported by the Deutsche Forschungsgemeinschaft and the Bundesministerium für Bildung und Forschung.

  1433-7851/01/4003-0552 $ 17.50+.50/0